Vol. 2: 131–149, 1992 | CLIMATE RESEARCH Clim. Res. | Published December 31

Sensitivity of wheat growth to increased air temperature for different scenarios of ambient CO_2 concentration and rainfall in Victoria, Australia – a simulation study

Y. P. Wang[1], Jr Handoko[2], G. M. Rimmington[2]

[1] CSIRO Division of Atmospheric Research, Private Bag No. 1, Mordialloc, Victoria 3195, Australia
[2] Plant and Soil Sciences Section, School of Agriculture and Forestry, University of Melbourne, Parkville, Victoria 3052, Australia

ABSTRACT: A wheat growth model that includes the direct responses of canopy photosynthesis and transpiration to elevated CO_2 and the response of crop growth to water stress has been developed and tested. Sensitivity analyses show that different cultivars have quite different responses to changes in ambient air temperature, ambient CO_2 concentration and rainfall. Because crops reach maturity earlier under higher temperature, an increase of 3 °C may not impose further water stress to growth of a wheat crop in Victoria, Australia. However shorter maturation time may lead to a net decrease in crop biomass accumulation and potential grain yield in some early maturing cultivars. It is suggested that selection of suitable cultivars is one of the key strategies for coping with climate change.

INTRODUCTION

Wheat yield in Australia has increased significantly on average over the last 50 yr as a result of technological improvement and genetic breeding (Elliot 1987), but the average yield is still much lower than that of many developed nations. Wheat production in Australia is strongly limited by the amount of rainfall in the growing season. In a region where average annual rainfall is less than 250 mm, wheat farming is considered to be economically marginal (Nix 1975).

Since the industrial revolution (mid-18th century), greenhouse gas concentrations have increased by an amount that is radiatively equivalent to about a 50 % increase in CO_2, although CO_2 itself has risen by 25 %, from 280 to 350 µmol mol^{-1} (Houghton et al. 1990). If global emissions continue at 1980's rates, it is expected that the CO_2 concentration will reach double pre-industrial levels (i.e. 560 µmol mol^{-1}) by 2060, and double present levels (i.e. 700 µmol mol^{-1}) by 2080. The associated global average surface warming is estimated to be about 1.5 °C above the present value by the middle of next century and 3 °C before 2100.

It is unlikely that the warming will be spatially uniform; land surfaces will warm more rapidly than the oceans, and high latitudes will warm more than the tropics. The global climate model (CSIRO4) developed by CSIRO Australia has indicated that the average temperature in Victoria (Fig. 1) could increase by 1 to 3 °C by about 2030, and rainfall could increase by up to 20 % in summer and decrease by up to 10 % in winter (Pittock & Whetton 1990).

In this study, we investigate whether a temperature increase will impose further water stress on wheat growth in Horsham, Victoria, and how different wheat cultivars respond to climate change using a process-based model of wheat growth. As temperature increase is caused by the enhanced greenhouse effect, and increased CO_2 concentration in the atmosphere contributes 55 % of the predicted global warming (Houghton et al. 1990), we will study the responses of crop growth to temperature increase for different scenarios of CO_2 concentration and rainfall.

Both CO_2 and air temperature can affect crop growth directly and indirectly. In a water-limited environment, the total amount of water available to the crop is an

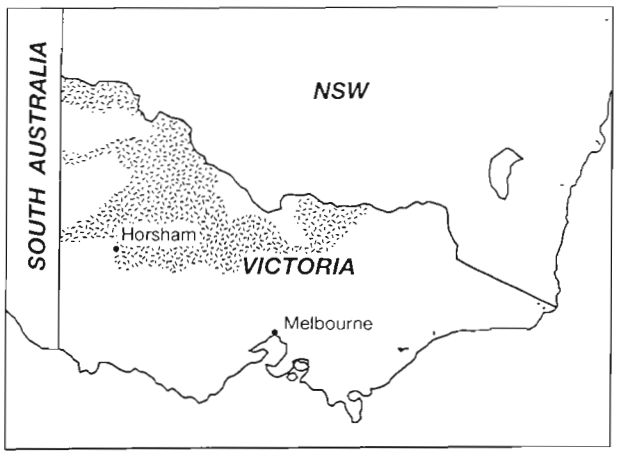

Fig. 1. Location of Horsham in Victoria, Australia. The wheat-growing region in Victoria is indicated as the shaded area

important determinant of grain yield. After anthesis, sufficient soil water supply is critical to achieving full yield potential. If soil water is depleted before anthesis, the crop will fail or only produce a low yield. Even though crop water-use efficiency will improve in the high CO_2 environment, the total water demand by the crop may not decrease as a result of the rapid crop canopy growth before anthesis (Gifford 1988). Increased temperature also increases potential evapotranspiration of the crop and may impose some additional water stress on the crop (Williams et al. 1988). On the other hand, increased temperature can accelerate crop development, and therefore reduce the total water used by the crop. The interactions between the increased CO_2 and air temperature on crop water use, growth and yield are difficult to clarify experimentally. A wheat growth model is used here to analyse the sensitivity of crop growth to changes in air temperature, CO_2 concentration and rainfall, and to help plant breeders identify cultivars suitable for the future climate.

DESCRIPTION OF THE MODEL

This model comprises 6 submodels. They are: (1) biomass production, (2) biomass allocation, (3) root extension, (4) soil evaporation and potential crop transpiration, (5) actual crop transpiration and (6) soil water balance. The model is developed from the wheat growth model of Handoko (1992), but it differs in the following ways:

(1) this model includes the stomatal, boundary layer and aerodynamic conductances in the calculations of canopy photosynthesis and transpiration;

(2) when water is not limiting to crop growth, biomass production is limited by the absorption of solar radiation, and is calculated using a process-based model of canopy photosynthesis, whereas Handoko's model assumes that the daily biomass production is proportional to the radiation absorption (Monteith 1977, Charles-Edwards et al. 1986). When water is limiting, the radiation-limited biomass production is reduced by the ratio of the actual and potential crop transpiration.

(3) the potential rate of crop transpiration is calculated using the Penman-Monteith equation, whereas Handoko's model calculates the potential rate of crop transpiration using a modified Penman equation (Meyer et al. 1987).

Crop growth rate is calculated in 2 steps. Firstly, it is calculated assuming that radiation absorption only is the limiting factor. Secondly, the radiation-limited growth rate is reduced by a water deficit factor defined as the ratio of the actual and potential rates of crop transpiration (Hanks 1974). Daily dry matter produced is partitioned into leaf, stem, spike and root in the biomass allocation submodel.

The model can be summarized by the following 3 key equations. Crop growth rate, dW/dt, is calculated as

$$dW/dt = aA_c f_w - rW \quad (1)$$

and

$$f_w = T/T' \quad (2)$$

$$T = \min\{T_x, T'\} \quad (3)$$

where W is crop biomass at time t; A_c is the photosynthetic carbon production of the crop in the absence of water stress; a is growth efficiency defined as amount of dry matter produced per mole of carbon; and r is the maintenance respiration coefficient of crop biomass. Crop transpiration, T, is taken as the smaller value of the transpiration limited by soil water (T_x) and the potential crop transpiration (T'). A_c, T_x, T' are calculated in Submodels 1, 4 and 5, respectively.

Daily growth rate of each biomass component (leaf, stem, root and spike) before anthesis is calculated in Submodel 2, and extension rate of roots is calculated in Submodel 3. Soil water balance is updated daily (Submodel 6). All the symbols are identified in Appendix I and a description of submodels is given in Appendix II.

Photosynthetic carbon production is simulated using a biochemical model of leaf photosynthesis. It has been shown that the response of crop growth to elevated CO_2 is quite consistent with the photosynthetic response (Gifford 1992). Submodels 1 and 2 have been validated against data from field gas exchange measurements and experiments in a CO_2-enriched glasshouse (Wang et al. 1991). A process-based model should be able to predict the plant response to climate change better than an empirical model, as the former is based on our understanding of biological processes

rather than empirical evidence which may become invalid in a new climate. So far, simulation of grain growth is still very empirical, therefore we decided to exclude grain growth from the model until a more mechanistic model of grain growth is developed. This is justified for a sensitivity study.

Development of the crop

Development of a crop is divided into phases separated by sowing, seedling emergence, start of stem extension, anthesis and physiological maturity. The rate of development depends on air temperature (T_a) or daylength (D_l), and is quantitatively evaluated using a variable, S_m, for each development phase [m = 1 (sowing to emergence), 2 (emergence to stem extension), 3 (emergence to anthesis) and 4 (anthesis to maturity)]. The overall development of the crop, S, is calculated from S_m.

The variable S_m is calculated for the development of a photoperiod-insensitive phase using

$$S_m = 0.25 \min \left\{ \int_{t_0}^{t} \frac{\delta_1 (T_a - T_m)}{U_m} dt, 1 \right\} \quad (4)$$

and for the development of a photoperiod-sensitive phase using

$$S_m = 0.25 \min \left\{ \int_{t_0}^{t} \frac{\delta_1 \delta_2 (T_a - T_m)(D_l - D_m)}{V_m} dt, 1 \right\} \quad (5)$$

where T_m is the base temperature of phase m; D_m is the base photoperiod for photoperiod-sensitive phase m; $\delta_1 = 1$ if T_a is greater than T_m, and = 0 otherwise; $\delta_2 = 1$ if D_l is greater than D_m, and = 0 otherwise; U_m is sum of degree days required for a photoperiod-insensitive phase; and V_m is sum of degree hours required for a photoperiod-sensitive phase to complete its development. t is days after sowing and t_0 represents the first day of the phase. For wheat cultivars used in this study, only development phase from emergence to anthesis (m = 3) is photoperiod sensitive.

Parameter S is calculated as

$$S = S_1 \quad \text{if} \quad S_1 < 0.25 \quad (6a)$$
$$S = S_1 + S_2 \quad \text{if} \quad S_2 < 0.25,\ S_1 = 0.25 \quad (6b)$$
$$S = S_1 + S_2 + S_3 \quad \text{if} \quad S_3 < 0.25,\ S_2 = 0.25 \quad (6c)$$
$$S = S_1 + S_2 + S_3 + S_4 \quad \text{if} \quad S_4 < 0.25,\ S_3 = 0.25 \quad (6d)$$

For very late maturing cultivars, such as UQ189 in this study, the rate of crop development from seedling emergence to anthesis is non-linearly related to air temperature or photoperiod (Angus et al. 1981), we use the non-linear relationship derived from the field data to model the phasic development from seedling emergence to anthesis (Stapper & Fischer 1990). For some early or moderately late maturing cultivars, the response is approximately linear within the temperature range 10 to 23 °C (Keulen & Seligman 1987), and may become significantly non-linear above 23 °C. However this non-linear part of the response is ignored in this simulation study for 2 reasons: (1) existing data are insufficient to enable us to derive a non-linear response function that is significantly better than the linear function, and (2) at Horsham, the vegetative phase of a wheat crop sown before August usually completes before November, when the daily mean air temperature usually is less than 20 °C. Excellent agreement between the predicted and observed crop phenology was obtained using a linear model of crop development for crops sown at different locations and sowing dates in Australia (Connor & Rimmington 1991). Under the assumption of a uniform warming by up to 3 °C, the vegetative growth of a wheat crop will complete before November if the crop is sown before August. The crop will experience very few days with daily mean air temperature above 23 °C before anthesis. Therefore the error resulting from the linear model of crop development is insignificant.

TEST OF THE MODEL

Details of the experiment from which data were used to test the model are explained elsewhere (Handoko 1992). Briefly, the experiment was conducted at the University of Melbourne Mt Derrimut Field Station, located 20 km west of Melbourne, during 1988. The experimental site consisted of a set of 27 drainage lysimeters (each 6 × 3 m^2 and 1.2 m deep). A wheat crop (Cultivar Matong) was sown on 27 May 1988 with 4 treatments using a combination of twice-weekly, drip irrigation and a rainout shelter. The treatments were: (R) rainfed with low rainfall after anthesis, (D) pre-anthesis water stress using the rainout shelter from 99 to 131 d after sowing followed by irrigation during 133 to 147 d after sowing, (I1) irrigation from 111 to 160 d after sowing in addition to the natural rainfall, and (I2) post-anthesis irrigation from 133 to 160 d after sowing. Measurements consisted of crop biomass, canopy leaf area index, phenology, soil water balance, and weather variables for model inputs (Fig. 2).

Soil water content of the rooting zone (1.2 m deep from the ground surface) was measured at least once every 2 wk using a neutron probe meter. Total amount of soil evaporation and crop transpiration was estimated from measurements once every fortnight for all the treatments with lysimeters and records of soil

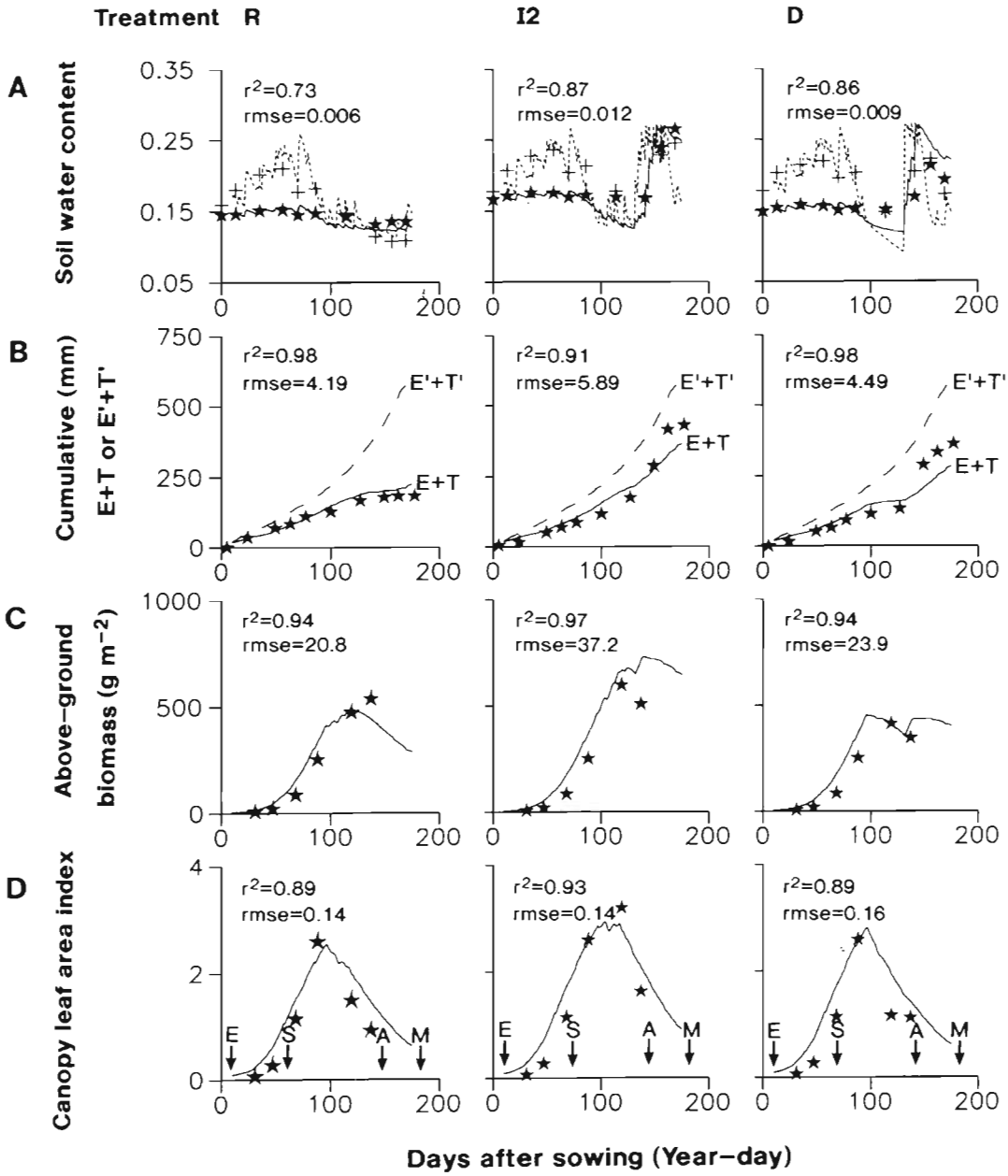

Fig. 2. Predicted (curve) and measured (points) values of: (A) soil water content (fraction by volume; solid curve is mean water content of whole soil profile, dotted curve is mean water content of top 20 cm soil), (B) cumulative total of soil evaporation (E) and crop transpiration (T), cumulative total of the potential soil evaporation (E') and potential crop transpiration (T'), (C) above-ground biomass and (D) canopy leaf area index from sowing to physiological maturity for Treatment R (rainfed), I2 (irrigation) and D (drought). Major crop development events are indicated on the lowest x-axes: 'E', for seedling emergence; 'S', stem extension; 'A', anthesis; 'M', physiological maturity. The crop in Treatment D was irrigated from 133 to 147 d after sowing and the crop in Treatment I2 was irrigated from 133 to 160 d after sowing

drainage. Plant samples were taken for measurements of the biomass of leaves, stems (including spikes and ears) 8 times from seedling emergence to physiological maturity except for rainfed treatments (7 times) since the crop died prematurely. Number of mature grains were counted for all treatments at crop harvest.

To test the model, values of all the parameters were chosen independently from the experimental data. Some parameters, such as the physical properties of the soil, were taken from measurements, and these have been indicated in Table 1. The agreement between the observed and the predicted values is good

Table 1. Values of parameters used in the simulation

Parameter	Value	Source	Unit
Seed sowing rate	7.5	Measured	g m^{-2}
a	21.4	(1)	g mol^{-1}
b_s at C_a = 350 µmol mol^{-1}	2.1×10^{-5}	(2)	m^3 J^{-1}
at C_a = 560 µmol mol^{-1}	1.7×10^{-5}	(2) + (3)	m^3 J^{-1}
at C_a = 700 µmol mol^{-1}	1.3×10^{-5}	(2) + (3)	m^3 J^{-1}
d_{max}	0.0075	Estimated	m
g_0	0.0005	(2)	m s^{-1}
k_b	0.4	(3)	–
k_d	0.8	(4)	–
k_r	3.0	(5)	m^{-1}
k_n	0.4	(8)	–
N	6		Layers
r_l (20 °C)	0.015	(6)	d^{-1}
r_s (20 °C)	0.010	(6)	d^{-1}
r_p (20 °C)	0.010	(6)	d^{-1}
r_r (20 °C)	0.015	(6)	d^{-1}
v_r	0.0022	(7)	m $°C^{-1}$ d^{-1}
$w_{min,i}$ (i = 1,2,..6)	0.1	Measured	m^3 m^{-3}
$w_{max,i}$	0.3	Measured	m^3 m^{-3}
Initial $w_{s,i}$ (at sowing)	0.2	Measured	m^3 m^{-3}
C_e	0.012	(8)	m
H_0	0.1	Measured	m
H_s	1.2	Measured	m
Q_l	2	(6)	–
Q_s	2	(6)	–
Q_p	2	(6)	–
Q_r	2	(6)	–
α_p	105	(10)	grains g^{-1}
β	0.00508	(8)	m $d^{-0.5}$
σ_l	0.0175	Measured	m^2 g^{-1}
σ_r	1000	(11)	m g^{-1}

Sources: (1) Penning de Vries et al. (1974); (2) Denmead & Miller (1975); (3) Morison & Gifford (1984); (4) Gallagher & Biscoe (1978); (5) Goudriaan (1977); (6) Keulen & Seligman (1987); (7) Ritchie et al. (1985); (8) Ritchie (1972); (9) O'Leary et al. (1985); (10) Fischer (1983); (11) de Marco (1990)

for all 4 treatments, but comparisons are only shown for 3 treatments in Fig. 2.

The model simulated the total amount of actual soil evaporation and crop transpiration very well. When irrigation was applied in Treatments I2 and D, the model predicted a slower increase in the total rate of soil evaporation and crop transpiration than observed. Disagreement between the model simulations and observations may result from (1) advection or (2) some errors in the measurements of $E + T$. It is known that advection can cause the latent energy to exceed the net radiation. Soon after irrigation, crop transpiration and soil evaporation could be strongly affected by advection not included in this model. After irrigation, the soil profile was estimated to be fully saturated. Percolation took place, and the rate of percolation changed with time. In the experiment, only the weekly totals of soil percolation were measured and daily percolation was assumed to be constant when the estimates of $E + T$ were derived from the lysimeter data. Therefore the percolation rate would be under-estimated soon after irrigation and $E + T$ would therefore be over-estimated.

The model also over-estimated the above-ground biomass for the crop in Treatment I2. The difference between the observed and predicted values was largest near anthesis. It was observed that the crop in Treatment I2 suffered from severe water stress, and some plants nearly died, as indicated in Fig. 2D by the drastic reduction in canopy leaf area index a few days prior to anthesis. Irrigation was then applied to relieve some plants from severe water stress, but was a little too late. The observed above-ground biomass did not recover soon after irrigation. The model could not simulate the plant death from severe water stress very well, and the simulated response to irrigation may be much quicker than the actual response in the field. Separation between dead and live plant material in the field is difficult, which may also contribute some difference between the observed and predicted above-ground biomass around anthesis.

This model was not intended to simulate the actual rate of grain growth. However, 2 variables that are closely related to grain yield were simulated in this model. These are the total number of grains at anthesis and the potential rate of grain growth. If water supply is not a limiting factor to the crop from anthesis to physiological maturity, the actual rate of grain growth approaches its potential rate (Fischer 1983). When the crop experiences water stress during grain-filling, a significant amount of stem reserves will be remobilized for grain filling (Gallagher et al. 1976). As a result of the dynamic relationship between sources (leaf photosynthate and stem reserve) and sinks (grains), grain growth is much less sensitive to soil water deficit than the growth of leaves and stems (Fischer 1979). Usually final grain yield is proportional to the above-ground biomass at anthesis or the number of grains at anthesis (Fischer 1983). As shown in Fig. 3, the model satisfactorily predicted the above-ground biomass at anthesis and total number of grains.

A comparison of the simulated potential grain yield and the observed yield is presented in Table 2. Because of the timely irrigation applied to the crop in Treatment I1, the ratio of the observed and the simulated potential grain yield is largest among the 4 treatments, and is close to the value obtained by Fischer (1979). The difference between the actual and potential grain yield results from water stress after anthesis and limitation of carbon

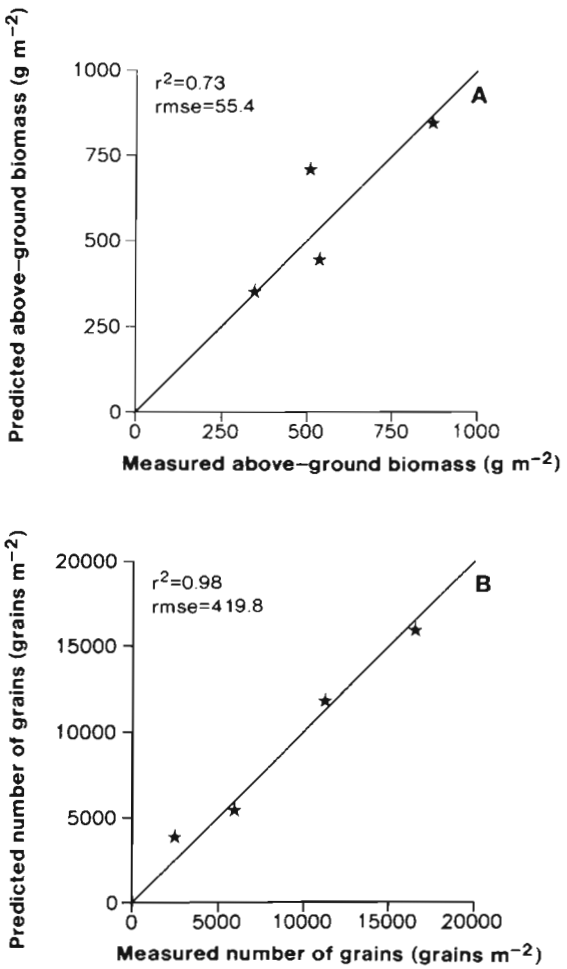

Fig. 3. (A) Predicted and measured above-ground biomass at anthesis, and (B) number of grains for all 4 treatments

supply for grain growth. The simulations showed that crops in Treatment I2 suffered from water stress to some degree before irrigation which resulted in a decrease in grain yield as compared with the crops in Treatment I1.

The model satisfactorily predicted the above-ground biomass at anthesis and total number of grains. The ratio of the observed grain yield to the simulated potential grain yield only varied between 0.5 to 0.8, depending on the degree of the post-anthesis water stress the crop experienced.

Table 2. Observed grain yield (1) and the simulated potential grain yield (2)

Treatment	(1) (g m^{-2})	(2) (g m^{-2})	(1)/(2)
R	78.1	153.0	0.51
I1	330.5	450.4	0.73
I2	176.5	333.3	0.53
D	54.1	101.0	0.54

GROWTH SENSITIVITY TO INCREASED AIR TEMPERATURE FOR DIFFERENT SCENARIOS OF CO_2 CONCENTRATION AND RAINFALL

The average wheat yield in Victoria from 1977 to 1988 was 1.73 tons ha^{-1} (Cribb 1989), which is similar to the average yield in the Horsham region. The average rainfall per annum is about 450 mm, monthly average maximum air temperature ranges from 13.4 (July) to 30.0 °C (January) and the monthly average minimum temperature varies from 3.5 (July) to 13.7 °C (January) at Horsham (see Fig. 4). The surrounding area is one of the major wheat production areas in Victoria (Fig. 1).

In this sensitivity study, 3 wheat cultivars were chosen: (A) Egret, (B) Matong and (C) UQ189. Cultivar A, a comparatively early maturing cultivar from New South Wales, is quite commonly planted in New South Wales and Victoria. Cultivar B is also quite commonly planted (Australian Wheat Board 1989) and Cultivar C is a late maturing cultivar from Queensland. Growth of early maturing cultivars is relatively more sensitive to temperature increase than that of late maturing cultivars. Comparative study of these 3 cultivars will illustrate the responses of different cultivars to climate change and help us to identify cultivars most suitable for the future climate.

An average present climate (control climate) for Horsham was simulated based upon historical records (Fig. 4). The simulated weather (dashed lines in Fig. 4) has the same range of seasonal behaviour as the historical record but differs in some monthly means. Two simulations were made using the model with para-

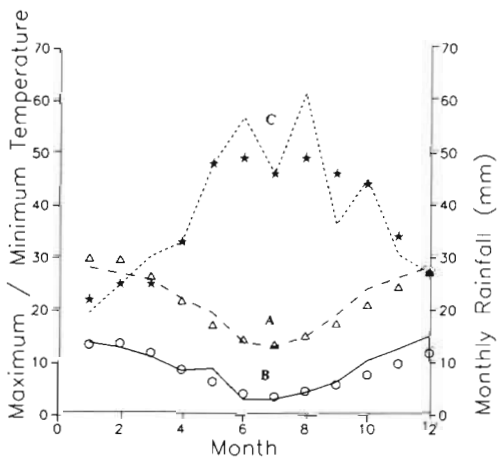

Fig. 4. Monthly means of the simulated (curves) and observed (points) climate variables: (A) maximum air temperature (°C), (B) minimum air temperature (°C) and (C) rainfall (mm mo^{-1}). The observed values were calculated from 29 yr of temperature data and 113 yr of rainfall data at Horsham (Bureau of Meteorology 1988)

Table 3. Phenological parameters in the simulations Subscripts refer to phase (m). Values of all parameters were taken from Rimmington & Connor (unpubl.), and were derived from field observations. *Degree days from sowing to anthesis are calculated using the relationship given by Stapper & Fischer (1990): $U_3 = 3205 - 29.13t_s + 0.1268t_s^2 - 0.00018t_s^3$, where t_s is day of sowing

Parameter	Cultivar			Unit
	Egret	Matong	UQ189	
T_1	3	3	3	°C
T_2	4	4	4	°C
T_3	2	2	3	°C
T_4	8	8	3	°C
D_2	6	6	•	h
U_1	89.7	93	87	degree day
U_2	307.1	281.6	315.0	degree day
V_3	4453.4	6838.0	•	degree hour
U_4	341.2	433.1	602	degree day

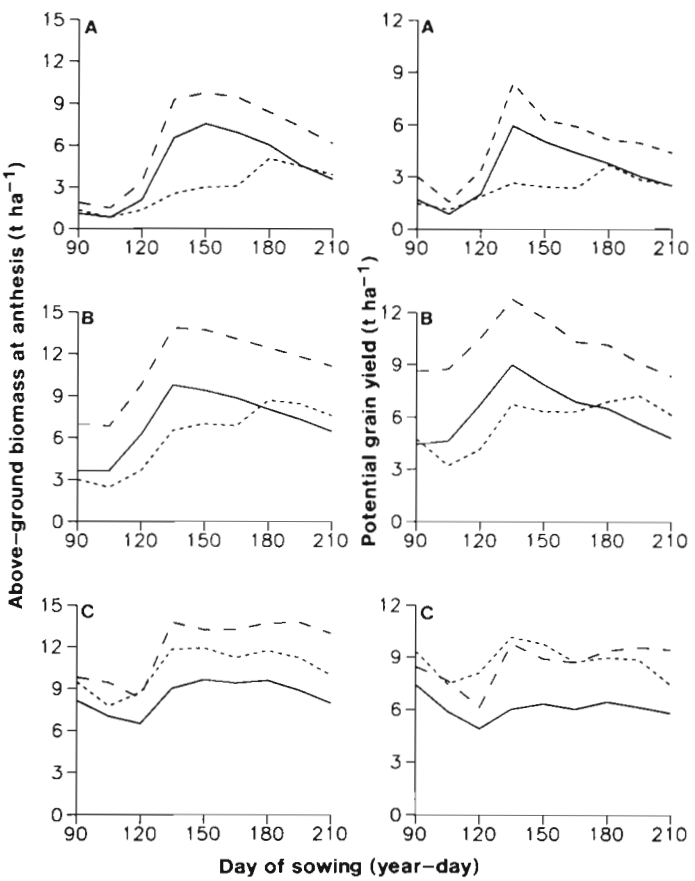

Fig. 5. Variations of the above-ground biomass at anthesis and potential grain yield for (A) Cultivar A (Egret), (B) Cultivar B (Matong) and (C) Cultivar C (UQ189) with day of sowing. Simulations were made for crops sown every 2 wk from year-day 90 to 210 for 3 different climate scenarios. Scenario 1: C_a = 350 µmol mol^{-1}, ΔT_a = 0 °C (———); Scenario 2: C_a = 700 µmol mol^{-1}, ΔT_a = 0 °C (– – –); Scenario 3: C_a = 700 µmol mol^{-1}, ΔT_a = 3 °C (-----)

meter values presented in Tables 1 & 3 for sensitivity analysis. Simulation 1 studies the response of crop growth to day of sowing for a temperature increase of 3 °C and CO_2 concentrations of 560 or 700 µmol mol^{-1} Simulation 2 studies the response of crop growth to a range of different climate scenarios for a crop sown at the optimum sowing day. The 2 simulations are complimentary.

Simulation 1

Simulations of crops sown once every 2 wk from year-day 90 to 210 were performed using 3 different climate scenarios [Scenario 1: control climate with ambient CO_2 concentration (C_a) of 350 µmol mol^{-1}; Scenario 2: control climate with C_a increased to 700 µmol mol^{-1}; Scenario 3: control climate with air temperature increased by 3 °C and C_a to 700 µmol mol^{-1}]. We simulated the amount of above-ground biomass at anthesis (W_a), the potential grain yield (W'_g), and the duration of crop growth, and the results are shown in Figs. 5 & 6.

Fig. 5 shows that the optimum sowing year-days for all 3 cultivars are between middle of April and early May. This is consistent with the current farming management practice at Horsham (Connor & Rimmington 1991). Though the sowing year-day in practice also depends on occurrence of opening rains. If a crop was sown before April, the crop would reach anthesis between August and September, and likely suffer from frost damage. For this reason, the predicted high potential grain yield for Cultivar C sown on year-day 90 will be significantly reduced if frost risk is considered in the model. Therefore the optimum sowing date for Cultivar C would be between late May and early June. For crops sown after April, the frost risk usually is quite small.

As shown in Fig. 5, an increase in C_a to 700 µmol mol^{-1} (Scenario 2) would increase W_a and W'_g for all 3 cultivars. The predicted increase in W'_g resulted from an increase in number of grains that was proportional to the spike dry weight at anthesis (see Appendix II). An increase in C_a had little effect on the optimum sowing year-days for all 3 cultivars.

If air temperature increased by 3 °C (Scenario 3), the optimum sowing year-day would be delayed by about 30 d for Cultivar A and about 50 d for Cultivar B, but little affected for Cultivar C. Doubling the present level of C_a would not compensate the losses resulted from a 3 °C increase in air temperature in W_a and W'_g for

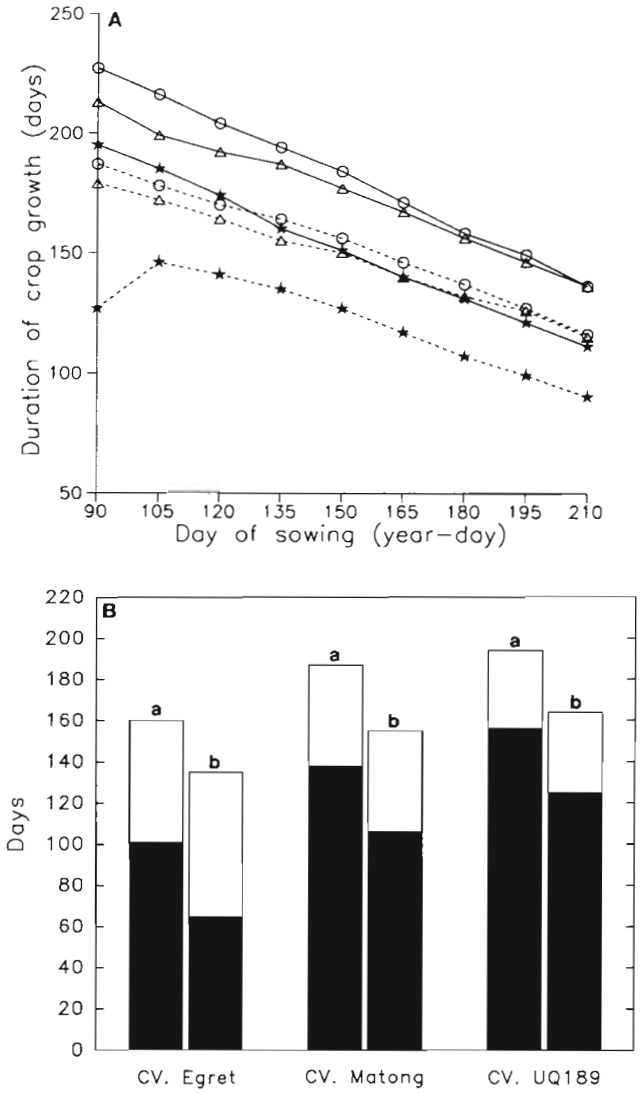

Fig. 6. (A) Duration of crop growth (from sowing to physiological maturity) for Cultivar Egret (★), Matong (△) and UQ189 (○) sown at different year-day under control climate (——) and a temperature increase by 3 °C (----); and (B) duration of crop growth from sowing to anthesis (black bars) and from anthesis to physiological maturity (open bars) for (a) control climate and (b) a temperature increase by 3 °C for 3 cultivars sown on year-day 135

Cultivars A and B if the crops were sown before year-day 180. However for Cultivar C, W_a was predicted to increase by 15 to 25 % and W'_g by 20 to 50 % if air temperature increased by 3 °C and C_a increased to 700 μmol mol^{-1}.

The responses to a doubling present level of C_a and an increase in air temperature by 3 °C differed between cultivars, as shown in Fig. 5. For Cultivar C, the beneficial effect of doubling present level of C_a (700 μmol mol^{-1}) would be large enough to counterbalance the detrimental effect of a temperature increase of 3 °C for a sowing day between 90 and 210 (Fig. 5C). For Cultivar A, doubling the present level of C_a would not be enough to cancel out the detrimental effects of an increase in air temperature of 3 °C, with the resultant reduction in both W_a and W'_g (Fig. 5A). If the sowing day was earlier than year-day 180 for Cultivar B, doubling present level of C_a would not counterbalance the detrimental effect of a 3 °C increase in air temperature. But if sowing date was later than year-day 180, doubling the present level of C_a would lead to fractional increases in both W_a and W'_g (Fig. 5B).

Temperature increase would have 2 major direct effects on W_a and W'_g. (1) A warming of 3 °C could increase the crop growth rate. For wheat, the optimum temperature for maximising crop growth rate per day was about 20 °C. (2) The duration of crop development would decrease with an increase in air temperature, and the total biomass production during the whole growth period would consequently be reduced. Therefore the optimum temperature for maximising W_a and W'_g would vary between 10 and 20 °C, depending on cultivars and other environmental variables. The temperature optimum of W_a and W'_g could also be quite different, as shown in Fig. 5B.

Fig. 6A shows that the duration of crop growth generally decreased with day of sowing. A temperature increase of 3 °C would result in a reduction of the duration of crop growth from sowing to physiological maturity by approximately 30 d for all 3 cultivars sown at different days of the year.

Fig. 6B shows that the response of the duration of vegetative and reproductive phases to a temperature increase by 3 °C. As a result of 3 °C warming, the crop developed faster, completed the vegetative growth earlier and experienced similar air temperatures during the reproductive growth as the crop grown under present climate conditions for Cultivars B and C. Therefore the durations of reproductive growth of Cultivars B and C were little affected by the warming. However for Cultivar A, a 3 °C warming would shorten the duration of vegetative growth from 101 to 65 d, and increase the duration of reproductive growth by 11 d. Therefore a 3 °C warming would result in the reproductive growth of Cultivar A in a cooler climate than the crop grown under present climate conditions. Cultivar A is an early-maturing cultivar, with canopy leaf area index never exceeding 2 during vegetative growth under the condition of 3 °C warming, therefore less solar radiation would be absorbed and less dry matter produced. This effect could multiply, and result in a massive reduction in the dry matter production at anthesis and grain numbers at anthesis, and consequently the potential grain yield, as shown in Fig. 5. For crops grown under elevated CO_2 conditions, it was just the opposite. The interaction between increased air temperature and ambient CO_2 concentra-

tion varies with the maturity type of the cultivar. For late-maturing cultivars, development rate of the crop was relatively less sensitive to temperature increase than the early-maturing cultivars, and therefore the beneficial effect of elevated CO_2 would counterbalance the detrimental effect of the increased temperature. Because the relationship between crop development rate and air temperature from seedling emergence to anthesis may deviate from the linear relationship assumed in this study at a temperature above 20 °C, we may have over-estimated temperature response, but the general conclusion about comparative responses of the 3 cultivars should still hold.

The effect of an increase in ambient air CO_2 concentration on total water use by the crop was quite small, as shown in Fig. 7. An increase in ambient CO_2 concentration would improve the crop water use efficiency (Gifford 1988), and also increase the canopy leaf area index. Therefore the total amount of water use by the crops grown under Scenarios 1 and 2 was similar for Cultivars Egret and Matong and for Cultivar UQ189 until 20 d before anthesis; this is consistent with some experimental observations (Gifford 1988). The differences in water stress suffered by Cultivars Egret and Matong during their vegetative growth also were quite small because of the compensation between a larger leaf area index and higher efficiency of water use for crops grown under Scenario 2, in agreement with some glasshouse studies (Gifford 1988). However this compensation was not so good for Cultivar UQ189 near anthesis. The crop grown under Scenario 2 suffered less water stress than the crop grown under Scenario 1.

Temperature increase could increase the potential canopy transpiration and also the root extension, therefore deeper soil water would be available for plant use. During the early stage of vegetative growth, the availability of soil water for plant use depended on the rooting depth and rooting density in the soil. Even though the canopy transpiration for the crop grown under Scenario 3 was larger, the water stress suffered by the crop was smaller than the crops grown under Scenario 1 or 2, because of greater extraction of soil water by the roots. Crops grown under Scenario 3 reached anthesis earlier, had a smaller canopy leaf area index, and therefore used less water before anthesis than the crops grown under Scenario 1 or 2, as shown in Fig. 7.

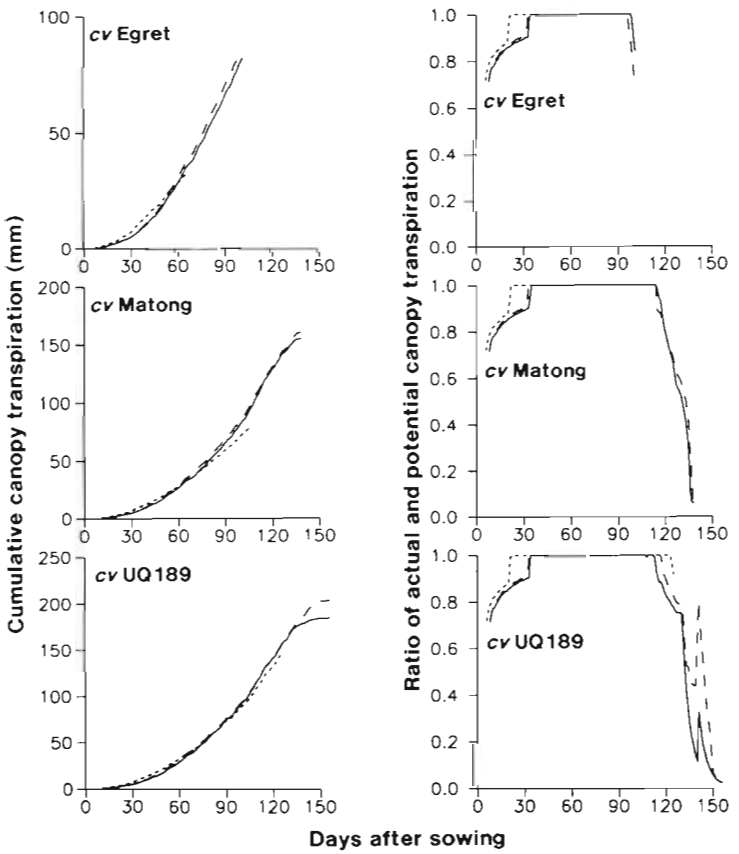

Fig. 7. Cumulative crop transpiration and ratio of actual and potential crop transpiration from emergence to anthesis for a crop sown on year-day 135 for 3 cultivars. Curve styles as in Fig. 5

Simulation 2

The amount of above-ground biomass and potential grain yield were simulated by varying the daily amount of rainfall by a fraction of −0.2 to 0.2, increasing the daily maximum and minimum temperatures equally by up to 3 °C (Pittock & Whetton 1990), and ambient CO_2 concentration from 350 to 560 and to 700 µmol mol^{-1}. The sensitivities of the above-ground biomass at anthesis and the potential grain yield of the crop sown at year-day 135 (the optimum sowing day for all 3 cultivars at the control climate; see Fig. 5), were calculated and results are shown in Figs. 8, 9 & 10. The relative change of W_a or W'_g was calculated as the difference between W_a or W'_g for a crop grown in a given climate scenario and that for a crop grown under the control climate (Scenario 1), divided by the value of W_a or W'_g for the crop grown under the control climate.

An increase in CO_2 concentration would be beneficial to crop growth of all cultivars, as shown in Figs. 8, 9 & 10. If there was no increase in air temperature when C_a increased from 350 to 560 and to 700 µmol mol^{-1}, the relative increase of W_a was more than 25 %, and the relative increase of W'_g was even larger, varying from 25 to 50 % for the 3 cultivars.

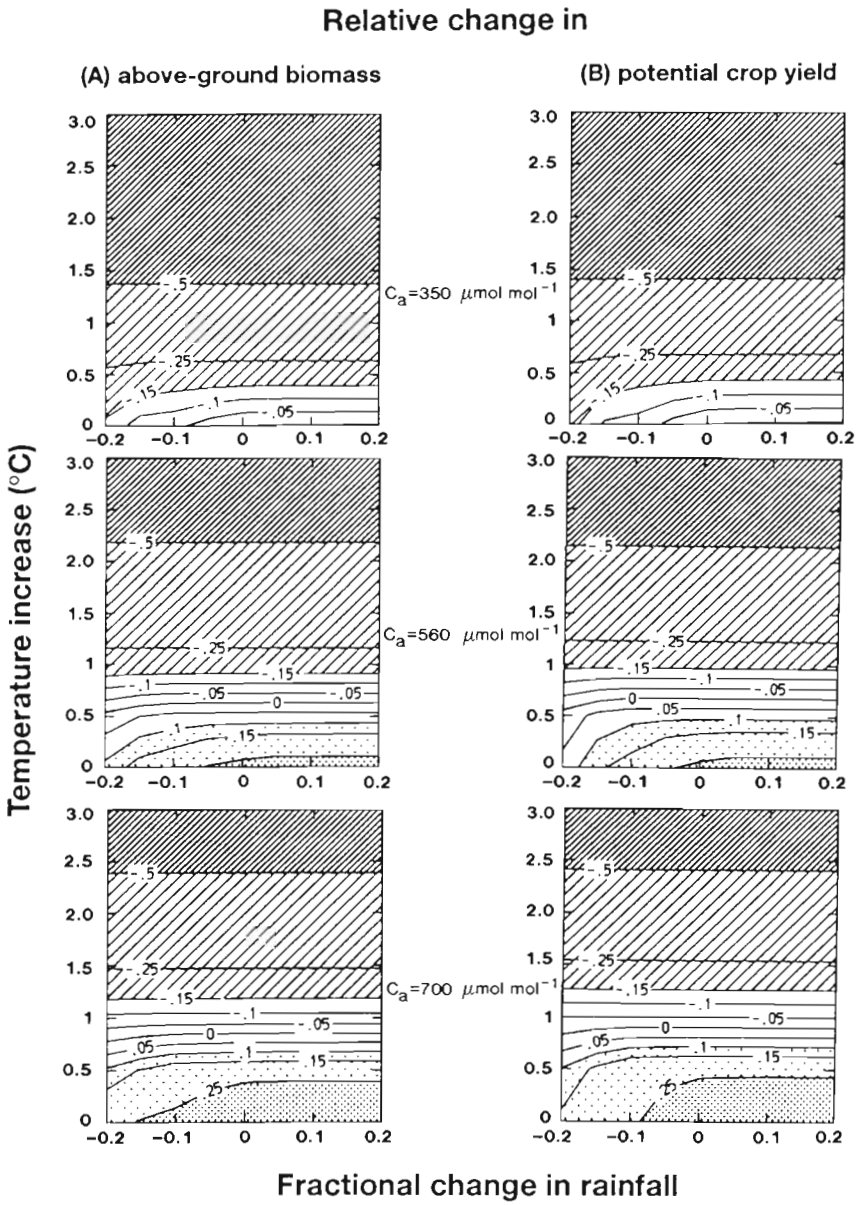

Fig. 8. Relative change in the above-ground biomass at anthesis and potential grain yield for wheat Cultivar A (Egret) planted at the optimum sowing date (year-day 135) for a warming of up to 3 °C and a fractional change of daily rainfall from −0.2 to 0.2 for ambient CO_2 concentrations of (a) 350 µmol mol^{-1}, (b) 560 µmol mol^{-1} and (c) 700 µmol mol^{-1}. In the contour map, isoline 0 represents no change in above-ground biomass as compared with the above-ground biomass simulated for control climate in Horsham with ambient CO_2 of 350 µmol mol^{-1}. −0.1 and 0.1 represent a 10 % decrease and a 10 % increase in the above-ground biomass, respectively. Above-ground biomass at anthesis and the potential grain yield at control climate condition are 652.9 and 595.5 g m^{-2}, respectively

For Cultivar A (Fig. 8), a temperature increase of 3 °C would result in a reduction of more than 50 % in W_a and W'_g. The sensitivities of both W_a and W'_g to warming were independent of the fractional change in rainfall from −0.2 to 0.2 if temperature increased by more than 1 °C. An increase in C_a from 350 to 560 and 700 µmol mol^{-1} would only partially counterbalance the detrimental effect of a temperature increase of 3 °C.

For Cultivar B, the responses of both W_a and W'_g to warming were not as great as for Cultivar A. At a C_a of 350 µmol mol^{-1}, if an increase in rainfall of >0.1 was accompanied by an increase in temperature of <0.5 °C, then small increases in W_a and W'_g were predicted with increasing rainfall. If the temperature increase was less than 1.5 °C and C_a was increased to 560 or 700 µmol mol^{-1}, then increases in W_a and W'_g of up to 50 % were also predicted, and these effects could be further enhanced by an increase in rainfall. If temperature increased by more than 2 °C, then decreases in W_a and W'_g were predicted, and these effects were independent of the change in rainfall.

For Cultivar C, the responses of W_a and W'_g were more complex than for Cultivars A and B. At C_a of 350 µmol mol^{-1}, W_a increased with a warming of up to 1.5 °C and then decreased while W'_g increased with a warming of up to 2 °C followed by a decrease. These findings are consistent with the average temperature difference between Horsham and Toowoomba, Queensland, where Cultivar C was bred. The average difference of mean air temperature is about 2.5 °C throughout May to December, the period of vegetative and reproductive growth of Cultivar C.

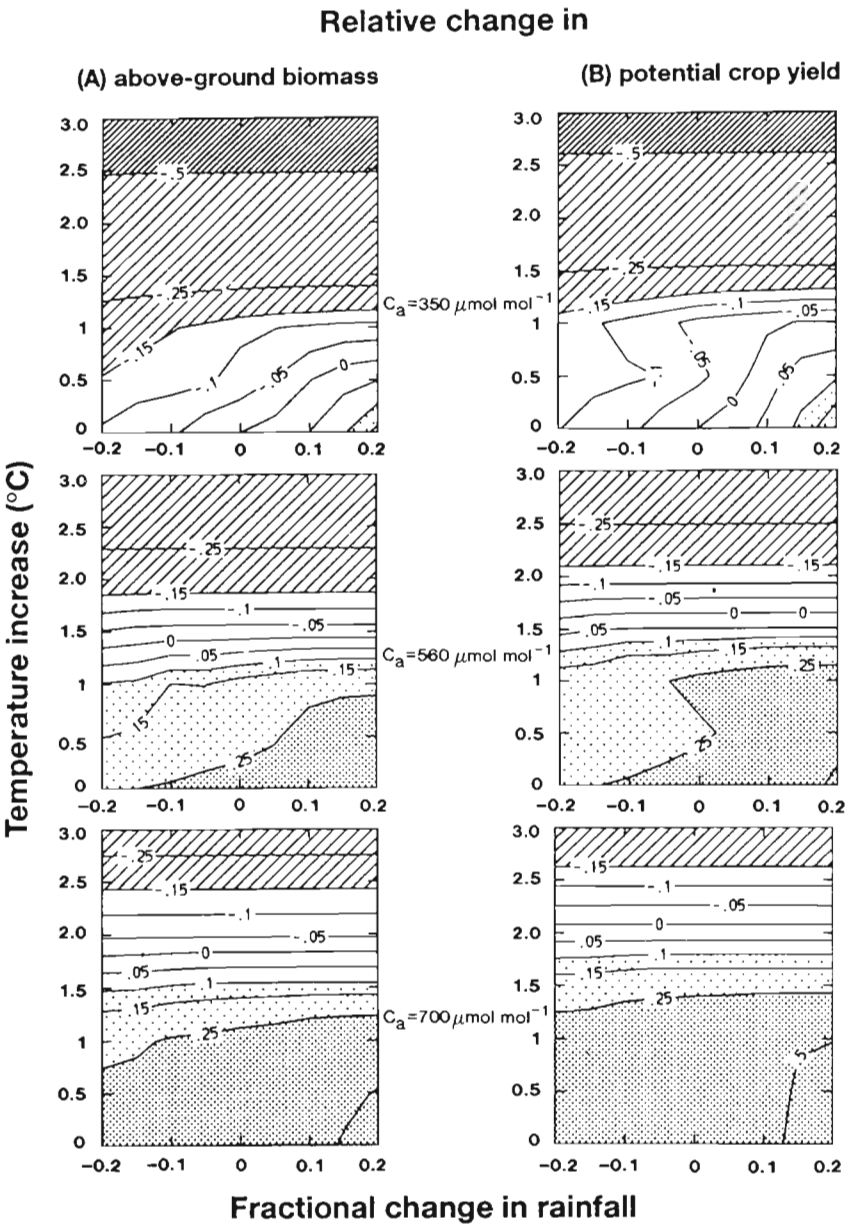

Fig. 9. As for Fig. 8, using Cultivar B (Matong). Above-ground biomass at anthesis and the potential grain yield at control climate condition are 977.3 and 898.3 g m^{-2}, respectively

To investigate the lack of sensitivity of W_a and W'_g to fractional changes in rainfall from −0.2 to 0.2 under a warming of more than 2 °C, canopy leaf area growth of Cultivar C from seedling emergence to anthesis was simulated for the following 3 climate scenarios: (a) C_a = 350 μmol mol^{-1}, and ΔT_a = 0; (b): C_a = 700 μmol mol^{-1}, ΔT_a = 1.5 °C; (c) C_a = 700 μmol mol^{-1}, ΔT_a = 3 °C. Two irrigation treatments were simulated for each climate scenario; one crop received no irrigation and the other was so well irrigated that supply of soil water never became limiting to crop growth. The results are shown in Fig. 11.

Under Scenario (a), the canopy leaf area index of a rainfed crop reached the maximum and then declined much more rapidly than for an irrigated crop. This was because the rainfed crop suffered from large soil water deficit that resulted in a more rapid leaf death than in the well-irrigated crop. Therefore, the dry matter production of a crop grown in Scenario (a) was very sensitive to the change in rainfall. Under Scenario (b), both the rainfed and irrigated crop reached a smaller maximum leaf area index, with anthesis 16 d earlier than the crops in Scenario (a), so the crops grown in Scenario (b) only suffered moderate water stress. Under Scenario (c), there was no difference in canopy leaf area growth between the rainfed and irrigated crop. A temperature increase of 3 °C caused the crop to reach anthesis about 30 d earlier, with a much smaller maximum leaf area index than crops grown in Scenario (a), resulting in much less water-use. Therefore supply of soil water was not

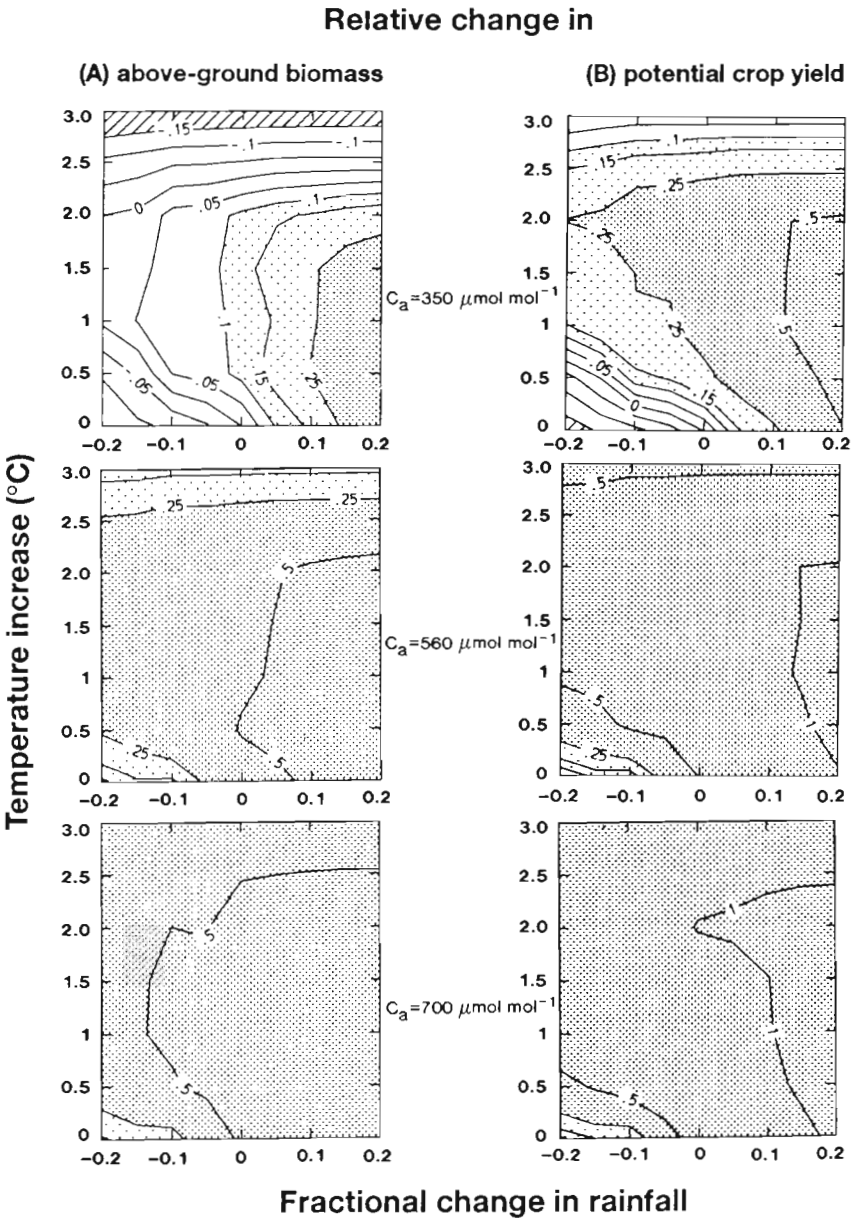

Fig. 10. As for Fig. 8, using Cultivar C (UQ189). Above-ground biomass at anthesis and the potential grain yield at control climate condition are 897.5 and 821.3 g m^{-2}, respectively

limiting to crop growth, and a fractional change in rainfall by −0.2 to 0.2 did not affect the above-ground biomass at anthesis and the potential grain yield of the crop grown in Scenario (c). However the effect of elevated CO_2 concentration on specific leaf area is not taken into account in this simulation. We may have over-estimated the effect of elevated CO_2 on canopy leaf area.

DISCUSSION

Global warming will affect wheat crops in 3 ways: through an increase in atmospheric CO_2 concentration, an increase in air temperature, and alternations to rainfall and evaporative demand. Global climate models predicted that by 2060, the average annual mean air temperature in Victoria will increase by up to 3 °C, and rainfall will increase by 20 % in summer and decrease by 10 % in winter as a result of global warming (Pittock & Whetton 1990). Temperature increase affects both crop growth and development as well as evaporative demand.

A crop model that accounts for the effects of CO_2, air temperature and soil moisture was used to simulate present conditions and the global warming conditions predicted for the Horsham region (Fig 1). The model incorporates the photosynthesis submodel of Farquhar & von Caemmerer (1982), integrated over the crop canopy, which responds to CO_2, incident solar radiation, and air temperature. Response to soil moisture is simulated with a submodel for crop transpiration and

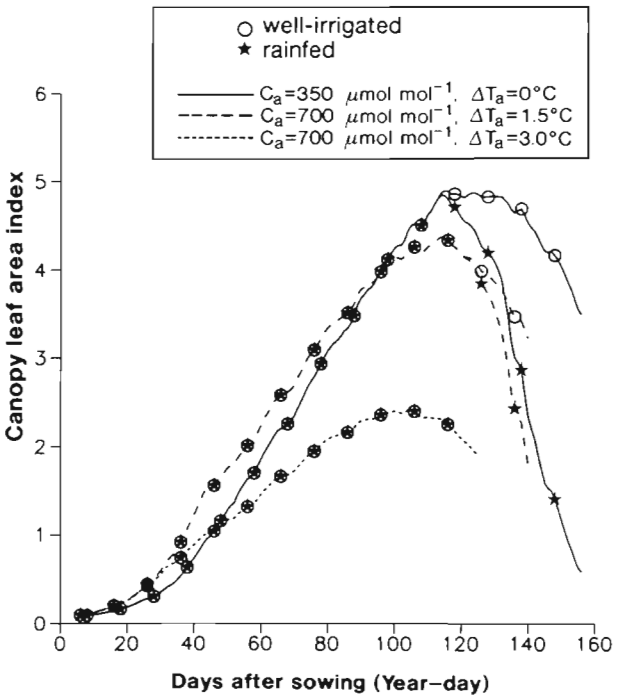

Fig. 11. Simulated canopy leaf area of Cultivar C (UQ189) grown under different environmental conditions (a) C_a = 350 μmol mol^{-1}, temperature increase (ΔT_a) of 0 °C; (b) C_a = 700 μmol mol^{-1}, ΔT_a = 1.5 °C and (c) C_a = 700 μmol mol^{-1}, ΔT_a = 3 °C, respectively. The crop was sown on year-day 135

development is simulated with a submodel derived from O'Leary et al. (1985). Weather and soil data for the Horsham region were used as inputs. Genetic specific coefficients for the development of 3 cultivars, (A) Egret, (B) Matong and (C) UQ189 (Table 3) were used in the simulations. This model does not account for nutrient limitations or the effects of weeds, pests or diseases.

Three scenarios were simulated for (1) present conditions (Fig. 4), (2) no increase in air temperature and a CO_2 concentration of 700 μmol mol^{-1} and (3) air temperature increased by 3 °C and a CO_2 concentration of 700 μmol mol^{-1}. The model predictions of present conditions agreed well with field observations (Table 2, Figs. 2 & 3) indicating that it is sufficiently reliable to make predictions of the impact of global warming on wheat crop. Scenario (2) allows investigation of the effects of doubling present CO_2 concentration. Scenario (3) combines the effects of doubling present CO_2 concentration and the associated temperature increase as predicted by the global climate models for the year 2080. An increase in average annual air temperature by 3 °C, as in Scenario (3), is equivalent to moving the wheat crop from Horsham to Narrabri in northern New South Wales using the assumption of a −0.45 °C (degree latitude)$^{-1}$ (Charles-Edwards et al. 1986).

The simulations indicated that the effect of increased air temperature by 3 °C was greater than that of doubling present CO_2 level (Fig. 5) for Cultivars Egret and Matong, while doubling present CO_2 level in Scenario 2 increased both above-ground biomass at anthesis and potential grain yield when temperature was increased as well (Scenario 3). Above-ground biomass at anthesis and potential grain yield fell below those for present conditions for crops sown up until early June. The simulations predicted that increased temperature would also delay the occurrence of maximum above-ground biomass at anthesis by approximately 30 and 50 d for Cultivars Egret and Matong, respectively (Fig. 5). The lower above-ground biomass at anthesis and potential grain yield values under Scenario (3) than under Scenario (2) suggested that doubling present CO_2 concentration and hence the increased canopy photosynthetic rate would not compensate for the detrimental effects of increased air temperature. On the other hand, above-ground biomass at anthesis and potential grain yield increased with increasing CO_2 concentration and air temperature for Cultivar UQ189 which apparently would be better suited to the enhanced greenhouse conditions in the Horsham region than existing cultivars.

The model predicted that increased temperature would alter the development pattern of each cultivar (Fig. 6B) but would not significantly alter either canopy transpiration or crop moisture deficit, as expressed by the ratio of actual and potential transpiration (Fig. 7). The vegetative growing period from sowing to anthesis was shortened by 30 to 35 d in each cultivar (Fig. 6B). The grain-filling period was lengthened by 10 d in Cultivar Egret but remained similar for Cultivars Matong and UQ189.

CONCLUSIONS

The simulations in this study took into account the effects of CO_2, air temperature, incident solar radiation and soil moisture on crop growth, water-use and development. They indicated that while doubling present atmospheric CO_2 concentration would lead to increases of between 28 and 43 % in above-ground biomass at anthesis and potential crop yield, a simultaneous increase in air temperature of just 3 °C would cause a reduction in above-ground biomass at anthesis and potential grain yield by up to 60 % for Cultivar Egret and 25 % for Cultivar Matong. This effect was mainly due to shortened vegetative growing periods, with no significant change in water deficit. In contrast the late-maturing cultivar UQ189, which is adapted to present conditions in southern Queensland, was predicted to have a higher above-ground biomass at anthesis and potential grain yield under the enhanced

greenhouse conditions. Therefore selection of suitable cultivars will be one of the key strategies to cope with climate change.

The present study has only considered changes to the average climate at Horsham, which effectively integrates large year-to-year variability. In the future, we plan to examine the sensitivity of inter-annual variability of wheat yield to various climate change scenarios. This may reveal more useful information for farmers concerned with risk analysis.

Acknowledgements. We thank the Australian Research Council, the Commonwealth Department of the Arts, Sport, the Environment, Tourism and Territories, and the Victorian Government for financial support to Y.P.W. We appreciate some constructive comments by Drs Ray Leuning and Miko Kirschbaum in Canberra, anonymous reviewers and colleagues from the Division of Atmospheric Research CSIRO, in particular Mr K. J. Hennessy.

LITERATURE CITED

Angus, J. F., Mackenzie, D. H., Morton, R., Schafer, C. A. (1981). Phasic development in field crops II. Thermal and photoperiodic responses of spring wheat. Field Crop Res. 4: 269–283

Australian Wheat Board (1989). Annual report 1988–1989. Melbourne

Barley, K. P. (1970). The configuration of the root system in relation to nutrient uptake. Adv. Agron. 22: 159–201

Bradford, K. J., Hsiao, T C. (1982). Physiological responses to moderate water stress. In: Lange, O. L., Nobel, P. S., Osmond, C. B., Ziegler, H. (eds.) Encyclopaedia of plant physiology, new series, Vol. 12B. Springer-Verlag, Berlin, p. 264–324

Brouwer, R. (1963). Some aspects of the equilibrium between overground and underground plant parts. Mededeling 213 van het I.B.S.: 31–39

Bureau of Meteorology (1988). Climate averages Australia. Australian Government Publishing Service, Canberra

Charles-Edwards, D. A., Doley, D., Rimmington, G. M. (1986). Modelling plant growth and development. Academic Press, London

Connor, D. J., Rimmington, G. M. (1991). Simulation models and analysis of variability in Australian wheat production. In: Geng, S., Cady, C. W. (eds.) Proceedings of climatic variation and changes: implications for agriculture in the Pacific Rim. Univ. of California, Davis, p. 27–44

Cribb, J. (1989). Australian agriculture: the complete reference on rural industry, Vol. 2. Moroscope Pty Ltd, Camberwell, Melbourne

Denmead, O. T., Miller, B. D. (1976). Field studies of the conductance of wheat leaves and transpiration. Agron. J. 68: 307–311

Davison, R. L. (1969). Effects of soil nutrients and moisture on root/shoot ratios in *Lolium perenne* L. and *Trifolium repens* L. Ann. Bot. 33: 571–577

de Marco, D. G. (1990). Effects of seed weight and seed phosphorus and nitrogen concentration on the early growth of wheat seedlings. J. exp. Agric. 30: 545–549

Elliot, B. (1987). Field crops. In: Connor, D. J., Smith, D. F. (eds.) Agriculture in Victoria. Australian Institute of Agricultural Science, Melbourne, p. 107–125

Farquhar, G. D., von Caemmerer, S. (1982). Modeling of photosynthetic response to environmental conditions. In: Lange, O. L., Nobel, P. S., Osmond, C. B., Ziegler, H. (eds.) Encyclopaedia of plant physiology, physiological plant ecology II, new series, Vol. 12B. Springer-Verlag, Berlin, p. 549–587

Fischer, R. A. (1979). Growth and water limitation to dryland wheat yield in Australia: a physiological framework. J. Aust. Inst. Agric. Sci. 45: 83–94

Fischer, R. A. (1983). Growth and yield of wheat. In: Smith, W. H., Banta, S. J. (eds.) Proceedings of symposium on potential productivity of field crops under different environments. International Rice Research Institute, Los Baños, Philippines, p. 129–154

Fischer, R. A. (1985). Number of kernels in wheat crops and the influence of solar radiation and temperature. J. agric. Sci. Camb. 105: 447–461

Gallagher, J. N., Biscoe, P. V., Hunter, B. (1976). Effect of drought on grain growth. Nature 264: 541–542

Gallagher, J N., Biscoe, P. V. (1978). Radiation absorption, growth and yield of cereals. J. agric. Sci. Camb. 91: 47–60

Gallagher, J. N. (1979). Field studies of cereal leaf growth. I. Initiation and expansion in relation to temperature and ontogeny. J. exp. Bot. 30: 625–634

Gerwitz, A., Page, E. R. (1974). An empirical mathematical model to describe plant root systems. J. appl. Ecol. 11: 773–781

Gifford, R. M. (1988). Direct effects of higher carbon dioxide concentrations on vegetation. In: Pearman, G. I. (ed.) Greenhouse, planning for climate change. CSIRO, Melbourne, p. 506–519

Gifford, R. M. (1992). Interaction of carbon dioxide with growth limiting environmental factors in vegetation productivity: implications for the global carbon cycle. Adv. Bioclim. 1: 25–58

Givnish, T. J. (1986). Optimal stomatal conductance, allocation of energy between leaves and roots, and the marginal cost of transpiration. In: Givnish, T. J (ed.) On the economy of plant form and function. Cambridge Univ. Press, Cambridge, p. 171–213

Goudriaan, J (1977). Crop micrometeorology: a simulation study. Simulation monograph, PUDOC, Wageningen

Handoko, Jr (1992). Analysis and simulation of nitrogen-water interactions of the wheat crop. Ph.D. thesis, Univ. of Melbourne

Hanks, R. J. (1974). Model for predicting plant yield as influenced by water use. Agron. J. 66: 660–665

Incerti, M., O'Leary, G. J. (1990). Rooting depth of wheat in the Victoria Mallee. Aust. J. exp. Agric. 30: 817–824

Houghton, J. T., Jenkins, G. J., Ephraums, J. J. (1990). Scientific assessment of climate change, the policymakers' summary of the report of working group I to the intergovernmental panel on climate change. Cambridge Univ. Press, Cambridge

Keulen, H. van, Seligman, N. G. (1987). Simulation of water use, nitrogen nutrition and growth of a spring wheat crop. Simulation monograph, PUDOC, Wageningen

Martin, P., Rosenberg, N. J., McKenney, M. S. (1989). Sensitivity of evapotranspiration in a wheat field, a forest, and a grassland to changes in climate and direct effects of carbon dioxide. Clim. Change 14: 117–151

McCree, K. J. (1974). Equations for the rate of dark respiration of white clover and grain sorghum, as functions of dry weight, photosynthetic rate and temperature. Crop Sci. 14: 509–514

Appendix I. Symbols and their definitions

a: growth efficiency expressed as grams of dry matter produced per mol of carbon (g mol C^{-1})
b_s: slope of the linear relationship between leaf stomatal conductance and radiation flux density on the leaf surface (m^3 J^{-1})
b_i: fraction of crop transpiration that can be supplied by plant root uptake in soil layer i
d_{max}: maximum effective root diameter (m)
d_r: root length density in the soil (m m^{-3})
$d_{r,i}$: mean root length density in soil layer i (m m^{-3})
e_i: fraction of crop transpiration that is available for root uptake in soil layer i
f_w: ratio of actual and potential crop transpiration
g_0: leaf stomatal conductance in the dark (m s^{-1})
g_b: sum of external aerodynamic and bulk boundary layer conductance (m s^{-1})
g_c: bulk canopy conductance (m s^{-1})
h: depth from soil surface (m)
h_i: depth from soil surface to bottom of soil layer i (m)
k_b: extinction coefficient of direct beam radiation
k_d: extinction coefficient of diffuse radiation
k_n: extinction of net radiation within crop canopy
k_r: empirical parameter to describe vertical root length density distribution in the soil (m^{-1})
l_r: root length per unit of ground area (m m^{-2})
n_g: number of grains (grains m^{-2})
p_i: percolation rate of soil water from soil layer i to layer $i + 1$ (m d^{-1})
r: maintenance respiration coefficient of crop biomass (d^{-1})
r_j: maintenance respiration coefficient of biomass component j (d^{-1})
r_a: external aerodynamic resistance (s m^{-1})
r_b: bulk boundary layer resistance (s m^{-1})
s: slope of temperature response curve of the saturated water vapour pressure (Pa K^{-1})
t: days after sowing (d)
t_0: first day of a phase (day of year from 1 January)
t_1: days after Stage 1 soil evaporation (d)
t_3: beginning of the linear grain filling phase in days after sowing (d)
t_4: end of linear grain filling phase in days after sowing (d)
t_a: days from sowing to anthesis (d)
t_e: days from sowing to seedling emergence (d)
t_s: day of sowing (day of year)
t': time of day (h)
u: wind speed at reference height (m s^{-1})
v_g': potential rate of grain growth (g $grain^{-1}$ d^{-1})
v_r: vertical velocity of the extension of rooting front in the soil (m $°C^{-1}$ d^{-1})
$w_{max,i}$: field capacity of soil layer i (m^3 m^{-3})
$w_{min,i}$: wilting point of soil layer i (m^3 m^{-3})
$w_{s,i}$: soil water content of soil layer i (m^3 m^{-3})
A_c: crop canopy photosynthetic carbon production (mol C m^{-2} d^{-1})
A_l: leaf photosynthetic rate (mol m^{-2} d^{-1})
C_a: ambient CO_2 concentration (µmol mol^{-1})
C_e: maximum stage 1 soil evaporation (m)
C_p: specific heat of air (J kg^{-1} K^{-1})
D_l: day-length (h)
D_m: base photoperiod for a photoperiod-sensitive development phase m (h)
D_t: time of day and night (s)
D_v: water vapour pressure deficit at the reference height (Pa)
E: soil evaporation rate (m d^{-1})
E': potential soil evaporation rate (m d^{-1})
F_b: beam fraction of incident solar radiation
H_0: sowing depth (m)
H_r: depth of the rooting zone (m)
H_s: depth of the soil (m)
I: canopy interception of rainfall (m d^{-1})
I_0: incident solar radiation flux density on the leaf surface (W m^{-2})
L: canopy leaf area index (m^2 m^{-2})
N: number of soil layers
Q_j: the Q_{10} coefficient for maintenance respiration of biomass component j
R: rainfall (m d^{-1})
R_n: net radiation above the canopy (W m^{-2})
S: parameter used to evaluate the overall phasic development of a crop
S_m: parameter used to evaluate the development of phase m (m = 1, 2, 3 and 4)
T: crop transpiration rate (m of H_2O m^{-2} d^{-1})
T_x: crop transpiration rate limited by soil water supply (m H_2O m^{-2} d^{-1})
T': potential crop transpiration (m H_2O m^{-2} d^{-1})
T_a: ambient air temperature at reference height (°C)
T_m: base temperature of phase m (°C)
U_m: degree days required for a photoperiod-insensitive phase to complete its development (degree day)
V_m: degree hours required for a photoperiod-sensitive phase to complete its development (degree hour)
W: crop biomass at time t (g m^{-2})
W_a: above-ground biomass of the crop at anthesis (g m^{-2})
W_g': potential grain yield (g m^{-2})
W_l: leaf dry weight (g m^{-2})
W_p': spike dry weight at anthesis (g m^{-2})
W_r: root dry weight (g m^{-2})
W_s: stem dry weight (g m^{-2})
α_p: number of grains per unit of spike dry weight at anthesis (grains g^{-1})
β: parameter to describe the change of stage 2 soil evaporation rate with time (m $d^{-0.5}$)
λ: latent heat of vapourisation (J kg^{-1})
η_j: allocation coefficient of photosynthetic dry matter production to biomass component j
η_l^*: allocation coefficient of dry matter production to the leaf when the crop does not suffer from water stress
η_r^*: allocation coefficient of dry matter production to the root when the crop does not suffer from water stress
γ: psychrometric constant (Pa K^{-1})
ρ: density of dry air (kg m^{-3})
σ_l: specific leaf area (m^2 g^{-1})
σ_r: specific root length (m g^{-1})

Appendix II. Description of growth submodels

Submodel 1. Biomass production

When water-supply is not limiting, dry matter production, dW/dt, is determined by photosynthetic carbon production and respiratory loss of the crop. The rate of dry matter production is reduced by a water deficit factor if the actual rate of crop transpiration is less than the potential rate of the crop transpiration. That is:

$$dW/dt = a A_c f_w - rW \qquad t \geq t_e \qquad \text{(II.1)}$$

where t is days after sowing; W is the total dry weight of crop biomass (g m^{-2}) at day t; t_e is days from sowing to seedling emergence; a is the growth efficiency defined as the amount of dry biomass produced per mol of carbon (Penning de Vries et al. 1974). Growth efficiency varies with the chemical composition of a plant organ, but this is ignored in the model. An average value is used in the simulation. A_c is the rate of canopy photosynthesis per unit ground area (mol m^{-2} d^{-1}) when photosynthetic carbon production is only limited by absorption of solar radiation; f_w is the water deficit factor; and r is the maintenance respiration coefficient of crop biomass (d^{-1}) (McCree 1974).

Following Hanks (1974), the water deficit factor, f_w, is calculated as:

$$f_w = T/T' \qquad \text{(II.2)}$$

where T and T' are the actual and potential rates of crop transpiration, respectively.

Crop biomass is separated into leaf (W_l), stem (W_s), spike (W_p) and root (W_r) before anthesis. The growth rate of each biomass component, W_j, (j = l, s, p and r for leaf, stem, spike and root, respectively) from seedling emergence to anthesis, is described by

$$dW_j/dt = a\,\eta_j A_c f_w - r_j W_j \quad j = \text{l, s, p and r}$$
$$\eta_l + \eta_s + \eta_p + \eta_r = 1 \qquad t < t_a \qquad \text{(II.3)}$$

where η_l, η_s, η_p and η_r are coefficients of biomass allocation to the leaves, stems, spikes and roots, respectively; and t_a is days from sowing to anthesis. Allocation coefficients vary during crop development (Fischer 1983), as shown in Fig. II.1.

Maintenance respiration rate of the biomass component, r_j, varies with ambient air temperature (T_a).

$$r_j(T_a) = r_j(20) Q_j^{(0.1[T_a - 2])}, \qquad j = \text{l, s, p and r} \qquad \text{(II.4)}$$

where Q_j is Q_{10} coefficient for respiration of biomass component j.

Canopy leaf area index, L, is related to leaf mass as

$$L = \sigma_l W_l \qquad \text{(II.5)}$$

where σ_l is specific leaf area (m^2 g^{-1}).

It is known that the rates of leaf initiation and expansion are strongly affected by air temperature (Gallagher 1979).

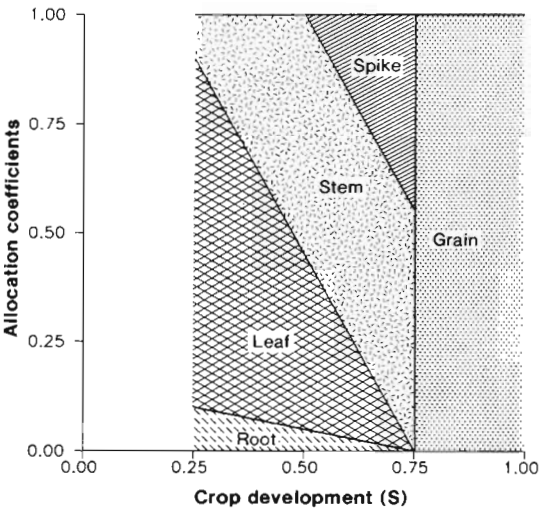

Fig. II.1 Variation of allocation coefficients during crop development for a crop that does not suffer from water stress. A parameter, S, is used to quantitatively describe crop development during each phase. The crop is sown at S = 0, and S = 0.25, 0.5, 0.75 and 1.0 correspond to seedling emergence, stem extension, anthesis and physiological maturity, respectively

As this model is a canopy model, growth response to air temperature at leaf scale is not considered.

A_c is calculated as

$$A_c = \int_0^{D_l} \int_0^{L} A_l \, dl \, dt' \qquad t > t_e \qquad \text{(II.6a)}$$

$$A_c = 0 \qquad t \leq t_e \qquad \text{(II.6b)}$$

where D_l is daylength; l is cumulative canopy leaf area index from canopy top; t' is time of day and A_l is the photosynthetic rate of the leaf (mol m^{-2} s^{-1}), calculated using a biochemical model of photosynthesis of Farquhar & von Caemmerer (1982) parameterized as in Wang et al. (1991).

Following Fischer (1983, 1985), the number of grains, n_g (grains m^{-2}), is assumed to be proportional to the spike biomass at anthesis, $W_p^{t_a}$ (g m^{-2}). That is

$$n_g = \alpha_p W_p^{t_a} \qquad \text{(II.7)}$$

Under elevated CO_2 conditions, dry matter production will increase, as the spike biomass anthesis, therefore more grains will be produced for achieving a higher potential grain yield than the crop grown under present conditions.

The actual rate of grain growth is not modelled. Only the potential rate of grain growth, v_g', is modelled here as a function of air temperature (see Fig. II.2) (Vos 1981).

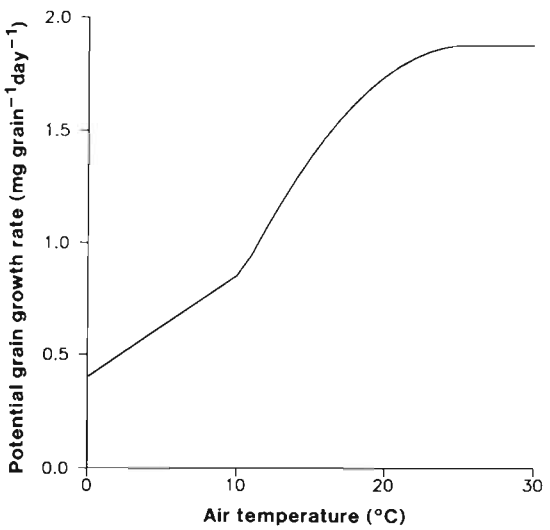

Fig. II.2. Variation of the potential rate of grain growth with air temperature. This curve is derived from the data of Vos (1981)

Potential grain yield (W_g') is then calculated as

$$W_g' = \int_{t_3}^{t_4} n_g v_g' \, dt$$

where t_3 and t_4 are the beginning and end of the linear grain filling in days, they are calculated according to the method outlined by Weir at al. (1984). Potential grain yield can only be achieved when supply of carbon for grain growth is not limiting and kernel abortion and water stress do not occur after anthesis (Fischer 1979).

Submodel 2. Biomass allocation

Allocation coefficients, η_l, η_s, η_p and η_r vary during crop development. If a crop does not suffer from any water stress ($f_w = 1$), relationships between the allocation coefficients and S, a parameter describing the phenological development of a crop, are shown in Fig. II.1.

Water stress can affect canopy growth, and results in an increase in the root-to-shoot biomass ratio (Brouwer 1963, Bradford & Hsiao 1982). Despite some recent progress (Schulze et al. 1983, Givnish 1986), there still is little consensus in describing quantitatively the response of the root-to-shoot ratio to water stress. After an extensive literature review, Wilson (1988) concluded that the response of carbon partitioning between root and shoot to water stress should be similar to that for nutrient deficiency, and this response is usually described by the functional equilibrium model (Davison 1969, Thornley 1972).

Following the concept of the functional equilibrium, biomass allocation coefficients, η_l and η_r for plants suffering from water stress are calculated as

$$\eta_l = \eta^*_l f_w \quad \text{(II.8a)}$$

$$\eta_r = \eta^*_r + \eta^*_l (1 - f_w) \quad \text{(II.8b)}$$

where η^*_l and η^*_r are the allocation coefficients to the leaf and root when the plant does not suffer from water stress, respectively (Fig. II.1). Allocation coefficients for stem and spike are assumed to be insensitive to water stress.

Submodel 3. Root extension

The total length of roots in the soil, l_r, is calculated as

$$l_r = \sigma_r W_r \quad \text{(II.9)}$$

where σ_r is the specific root length (m g^{-1}).

The density of root length at a depth of h in the soil is $d_r(h)$. Variation of root length density in the soil is assumed to be an exponential function (Gerwitz & Page 1974, Incerti & O'Leary 1990). The root density above the depth of the sowing (H_0) or below the rooting depth (H_r) is assumed to be zero. By definition, the density of root length in the rooting zone is given by:

$$d_r(h) = d_r(H_0)\exp[(-k_r(h - H_0)] \qquad H_0 \le h \le H_r \quad \text{(II.10)}$$

k_r is an empirical parameter.

The vertical velocity of rooting front extension in the soil, dH_r/dt, is calculated as (O'Leary et al. 1985):

$$dH_r/dt = v_r(T_a - 4) \qquad H_r < H_s, \quad T_a > 4\ °C \quad \text{(II.11a)}$$

$$dH_r/dt = 0 \qquad \text{otherwise} \quad \text{(II.11b)}$$

H_s is the depth of soil, and v_r is an empirical parameter.

Submodel 4. Soil evaporation and potential crop transpiration

The potential rate of soil evaporation, E', is calculated as follows (Ritchie 1972):

$$E' = \exp(-k_n L) \int_0^{D_t} \frac{s R_n + [0.64(1 + 0.54u)]D_v}{\lambda(s + \gamma)} \, dt' \quad \text{(II.12)}$$

where s is the slope of temperature response curve of the saturated vapour pressure at air temperature T_a; R_n is the net radiation above the canopy; u is mean wind speed at the reference height (2 m above the ground surface); D_v is the water vapour pressure deficit at the reference height; λ is the latent heat of vapourization of water; and γ is the psychrometric constant. D_t is the time of day and night in seconds (1 d = 86400 s). The radiation term, sR_n, is usually much greater than the second term $(0.64(1 + 0.54u)D_v)$ in Eq. II.12. The exponential term outside the integral, $\exp(-k_n L)$, is used to reduce the net radiation and the wind speed above the canopy to the respective values above the soil surface. To keep the model simple, the attenuations of wind speed and net radiation by the crop canopy are assumed to be the same. This exponential function has been proved to be a reasonable approximation (Tanner & Jury 1976).

The actual rate of soil evaporation, E, is calculated using Ritchie's method (1972). The process of soil evaporation

can be separated into 2 stages. During Stage 1, E is calculated as

$$E = E' \tag{II.13}$$

During Stage 2, the actual daily rate of soil evaporation, E, is calculated as

$$E = \beta(\sqrt{t_1} - \sqrt{t_1 - 1}) \tag{II.14}$$

where t_1 is days after the Stage 1 evaporation. Stage 1 soil evaporation is terminated once the water deficit of the top soil layer exceeds a critical value, C_e. Both C_e and β are specific to soil type.

The potential rate of crop transpiration, T', is calculated using the Penman-Monteith equation assuming soil water supply is not limiting to crop transpiration.

$$T' = \int_0^{D_1} \frac{sR_n + \rho C_p D_v g_b}{\gamma[s + \gamma(1 + \frac{g_b}{g_c})]} \, dt' \tag{II.15}$$

The time step for the integration is 1 h. ρ is the density of the dry air and C_p is specific heat of the air. s, g_b, g_c are calculated from the hourly means of the independent variables. g_b is calculated as

$$g_b = \frac{1}{r_a + r_b} \tag{II.16}$$

where r_a is the external aerodynamic resistance, and r_b is bulk leaf boundary layer resistance. They are calculated according to methods outlined by Martin et al. (1989).

Bulk canopy conductance, g_c, is calculated as (Denmead & Miller 1976)

$$g_c = g_0 L + b_s I_0[F_b(1 - \exp(-k_b L)) + (1 - F_b)(1 - \exp(-k_d L))] \tag{II.17}$$

where g_0 is the stomatal conductance of the leaf in the dark, and b_s is the slope of the linear relationship between the stomatal conductance and radiation flux density on the leaf surface. b_s varies with the ambient CO_2 concentration (see Table 1). k_b and k_d are extinction coefficients of direct beam and diffuse radiation, respectively. F_b is direct beam fraction of incident radiation and I_0 is the flux density of incident solar radiation above the canopy (W m^{-2}).

Submodel 5. Actual crop transpiration

When soil water supply is limiting to crop transpiration, the actual crop transpiration, T, is less than the potential crop transpiration given by Eq. II.15. Calculation of actual crop transpiration limited by soil water supply is described as follows.

Soil depth H_s was vertically divided into N layers. For each layer, supply of soil water for canopy transpiration depends on the relative availability of soil water (b_i) and the ability of roots within the layer to take up the available water (e_i). Calculation starts from the top layer ($i = 1$), and then proceeds downwards until the total amount of soil water available for crop transpiration is equal to the potential rate of crop transpiration given by Eq. II.15. If the total amount of available soil water for crop transpiration of N layers is less than the potential rate of crop transpiration, then the actual rate of crop transpiration is equal to the total amount of extractable soil water of the soil (T_x).

For soil layer i, the amount of extractable soil water by the plant roots, T_i, is taken as the smaller value of the amount of available soil water ($T'b_i$) and amount of water that can be taken up by the roots ($T'e_i$). That is

$$T_i = \min\{T'b_i, T'e_i\} \tag{II.18}$$

b_i is calculated as

$$b_i = 1.0 \quad \text{if} \quad w_i \geq 0.4 \tag{II.19a}$$

$$b_i = 2.5w_i \quad \text{if} \quad w_i < 0.4 \tag{II.19b}$$

$$w_i = \frac{w_{s,i} - w_{\min,i}}{w_{\max,i} - w_{\min,i}}$$

$w_{s,i}$ is the soil water content of soil layer i, and $w_{\min,i}$ and $w_{\max,i}$ are the wilting point and field capacity of soil layer i, respectively.

e_i is a function of root length density. Following Barley (1970), e_i is calculated as

$$e_i = \max\{0, 1 - \frac{1}{d_{\max}\sqrt{\pi d_{r,i}}}\} \tag{II.20}$$

where d_{max} is the maximum effective root diameter as defined by Barley (1970) and $d_{r,i}$ is the mean density of root length in soil layer i.

Crop transpiration limited by soil water, T_x, is calculated as

$$T_x = \sum_{i=1}^{N} T_i \tag{II.21}$$

Submodel 6. Soil water balance

The soil water balance was calculated daily for each of N layers. Change in soil water of the top layer (or surface layer), $\Delta w_{s,1}$ is

$$\Delta w_{s,1} = (R - I - p_1 - E - T_1)/h_1 \tag{II.22}$$

where R is rainfall; I is canopy interception; p_1 is percolation from the top layer; T_1 is the water depletion due to crop transpiration from the top layer; and h_1 is the depth of the top layer.

Change in soil water of the other layers, $\Delta w_{s,i}$ ($i = 2,3,...N$) is given by:

$$\Delta w_{s,i} = (p_{i-1} - p_i - T_i)/(h_i - h_{i-1}) \tag{II.23}$$

where h_i is the depth of soil layer i from the soil surface.

Canopy interception of rainfall, I (m d^{-1}), is calculated as (Zinke 1967)

$$I = \min(0.00127, 0.00042L) \tag{II.24}$$

where L is canopy leaf area index.

The rate of soil water percolation of layer i, p_i, ($i = 1,2,..N$) is calculated as

$$p_i = \max\{0.0, (w_{s,i} + \Delta w_{s,i} - w_{\max,i})(h_i - h_{i-1})\} \tag{II.25}$$

Meyer, W. S., Dunin, F. X., Smith, R. G., Shell, G. S. G., White, N. S. (1987). Characterizing water use by irrigated wheat at Griffith, New South Wales. Aust. J. Soil Res. 25: 499–515

Monteith, J. L. (1977). Climate and efficiency of crop production in Britain. Phil. Trans. R. Soc. Lond. Ser. B 281: 277–294

Morison, J. I. L., Gifford, R. M. (1984). Plant growth and water use with limited water supply in high CO_2 concentrations. I. Leaf area, water use and transpiration. Aust. J. Pl. Physiol. 11. 361–374

Nix, H. A. (1975). The Australian climate and its effects on grain yield and quality. In: Lazenby, A., Matheson, E. M. (eds.) Australian field crops, Vol. I, Wheat and other temperate cereals. Angus and Robertson, Sydney, p. 183–226

O'Leary, G. J., Connor, D. J., White, D. H. (1985). A simulation model of the development, growth and yield of the wheat crop. Agricult. Syst. 17: 1–26

Penning de Vries, F. W. T., Brunsting, A. B., Laar, H. H. van (1974). Products, requirements and efficiency of biological synthesis, a quantitative approach. J. theor. Biol. 45: 339–377

Pittock, A. B., Whetton, P. H. (1990). Regional impact of the enhanced greenhouse effect on Victoria. Annual report, 1989–90. CSIRO Division of Atmospheric Research

Ritchie, J. T (1972). Model for predicting evaporation from a row crop with incomplete cover. Water Resources Res. 8: 1204–1213

Ritchie, J. T., Godwin, D. C., Otter-Nacke, S. (1985). CERES-Wheat. A simulation model of wheat growth and development. Texas A & M Univ. Press, College Station

Schulze, E.-D., Schilling, K., Nagarajah, S. (1983). Carbohydrate partitioning in relation to whole plant production and water use of *Vigna unquiculata* (L.) Walp. Oecologia 58: 169–177

Stapper, M., Fischer, R. A. (1990). Genotype, sowing date and plant spacing influence on high-yielding irrigated wheat in southern New South Wales. I. Phasic development, canopy growth and spike production. Aust. J. Agric. Res. 41: 997–1019

Tanner, C. B., Jury, W. A. (1976). Estimating evaporation and transpiration from a row crop during incomplete cover. Agron. J. 68: 239–243

Thornley, J. H. M. (1972). A balanced quantitative model for root:shoot ratios in vegetative plants. Ann. Bot. 36: 431–441

Vos, J. (1981). Effects of temperature and nitrogen supply on post-floral growth of wheat; measurements and simulations. PUDOC, Wageningen

Wang, Y. P., Gifford, R. M., Farquhar, G. D., Wong, S. C. (1991). Direct effect of elevated CO_2 on canopy development of a wheat crop from sowing to anthesis: a model assessment. In: Geng, S., Cady, C. W. (eds.) Proceedings of climatic variation and changes: implications for agriculture in the Pacific Rim. Univ. of California, Davis, p. 19–26

Weir, A. H., Bragg, P. L., Porter, J. R., Rayner, J. H. (1984). A winter wheat crop simulation model without water or nutrient limitations. J. agric. Sci. Camb. 102: 371–382

Williams, G. D. V., Fautley, R. A., Jones, K. H., Steward, R. B., Wheaton, E. E. (1988). Estimating the effects of climatic variation on agriculture in the Saskatchewan, Canada. In: Parry, M. L., Carter, T R., Konijn, N. T (eds.) The impact of climatic variations on agriculture, Vol. 1, Assessments in cool temperate and cold regions. Kluwer, Dordrecht. p. 723–868

Wilson, J. B. (1988). A review of evidence on the control of shoot:root ratio, in relation to models. Ann. Bot. 61: 433–449

Zinke, P. J. (1967). Forest interception studies in the United States. In: Sopper, W. E., Lull, H. W. (eds.) Forest hydrology. Pergamon, Oxford, p. 137–161

Editor: T Oikawa

Manuscript first received: February 17, 1992
Revised version accepted: November 18, 1992